

Damage Detection Using Time-frequency Decay-rate based Features

Portia Banerjee
Global Research and Development
General Motors, Warren, MI 48092
Email: banerj20@egr.msu.edu

Debejyo Chakraborty
Global Research and Development
General Motors, Warren, MI 48092
Email: debejyo.chakraborty@gm.com

Teresa Rinker
Global Research and Development
General Motors, Warren, MI 48092
Email: teresa.rinker@gm.com

Abstract—Some automotive components, for instance a clutch housing, need to fit the assembly (dimensional constraint), and must be perfectly weight balanced for proper functioning (functional fidelity), which could be achieved by removing material from the body (relaxed geometry). While such mission critical components require 100% inspection, current non-destructive methods are often inadequate, trying to trade-off cycle time with inspection thoroughness. In this paper, a non-destructive global structural damage detection method has been demonstrated at its infancy, to be fast, accurate, and immune to inconsistent resonant frequencies which is an outcome of relaxed geometry. This method requires a traditional wide band exogenous acoustic excitation of the component being evaluated, followed by a joint time-frequency characterization of the response such that it is immune to dominant modal frequencies. A quadratic discriminant analysis on the time-frequency features successfully detected all damaged samples and falsely identified 1 among the 6 healthy samples available for testing, as damaged.

Index Terms—Damage detection, time-frequency, spectrogram, quadratic discriminant analysis, manufacturing

I. INTRODUCTION

A 100% quality inspection in a large volume manufacturing is challenging, especially when the inspection involves non-observable parameters of the component. Consider making a clutch housing for a car as an example. Aluminum is cast to the desired geometry and then machined for dimensional accuracy and weight balancing. The dimensions of this component can easily be verified, but not the existence of internal cracks. These cracks are a product of process anomaly of the casting and machining process. To address product reliability, such components are often engineered with a significant safety margin, which is a cost driver. In addition, tests like the spin test, eddy current inspection [1], [2] and dye penetrant inspection tests [3] are used as end-of-line quality check, which have their own shortcomings [4]. In the spin test, the component is rotated to a specified rpm, and if it does not yield, it passes. Eddy current is a localized test that takes up a significant portion of the cycle time for a thorough inspection, and the dye penetrant test works for substantial cracks on accessible and visible surfaces.

While there are several options of non-destructive inspection, like ultrasonic inspections [5], impedance-based methods [6], time-series analysis [7], statistical pattern recognition [8], and modal analysis [9] based methods, most have



Fig. 1. Classification system for crack damage detection in clutch housings.

at least one of the following concerns: requires statistically significant baseline training data, has high cycle time, performs local interrogation only, is too expensive, requires complex fixturing, relies on modal frequencies, sensitive to variations between samples being tested, etc.. In this paper, we have described a vibration based non-destructive inspection technique that overcomes these challenges for detecting crack damage. This method produced acceptable results when applied to the inspection of a limited number of clutch housing samples that were available for this experiment. In this paper, we have described this method and discussed the obtained results.

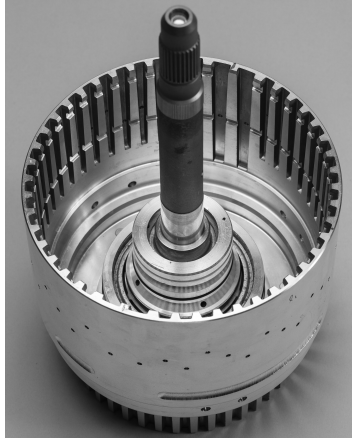
The remainder of this paper is organized as follows. The following section, Section II, describes the theoretical background and establishes the necessary mathematical foundation. Section III illustrates the experimental setup, discusses the acquired data and presents the obtained results. Finally, Section IV presents our conclusion and provides a natural direction for this research.

II. BACKGROUND

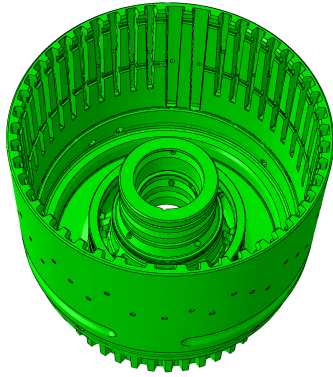
Non-destructive inspection using signals processing techniques usually involve the steps shown in Fig. 1. An exogenous input is used to excite the structure. In this document we will refer to this action as *pinging*. The response signal is then observed and analyzed. Relevant features from it is calculated, which is used to determine a healthy sample from a damaged one with the use of a classifier.

A. Component

Automotive clutch housing samples, as shown in the Fig. 2(a), are manufactured in several stages, among which molding and machining are the most significant. Internal cracks are known to develop primarily due to (a) temperature instability during the casting process, (b) material impurity, and (c) machining process anomaly. An ideal component



(a) Photograph.



(b) Finite element rendering.

Fig. 2. Clutch housing.

Fig. 3. Non-uniform removal of material in clutch housings (M_1 , M_2 and M_3 from left to right) used in experiment.

(Fig. 2(b)) has the first 7 vibration modal frequencies under 1 kHz. When the clutch housing is pinged near the free end of the barrel, an exponentially decaying sound that is primarily a composite of all modal frequencies, is audible. This constitutes the acoustic signature of this component. In production, the samples are hardly identical. Note the variation in geometry due to removal of material near the base of clutch housing samples, as shown in Fig. 3. This is done for load balancing, and causes shifts in the modal frequencies. Such uniqueness introduce significant sample-to-sample variation in modal frequencies, and thus the acoustic signature.

B. Signal Analysis

The acoustic signature of the clutch housing could be modeled as a linear combination of exponentially windowed

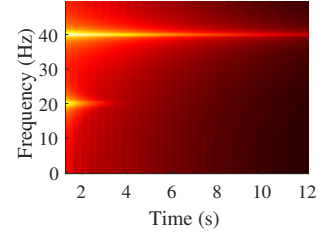


Fig. 4. Spectrogram of a synthetic response.

sinusoidal waves

$$x(t) = \sum_{n=1}^N a_n e^{-\lambda_n t} \cos(2\pi f_n t + \phi_n), \quad (1)$$

where t represents time in seconds, N is the arbitrary number of components, a is the amplitude, λ is the decay rate of the exponential window, f is the frequency in Hz, and ϕ is phase. Damage is manifested as a shift in frequencies (the higher the mode, the more the shift), and decay rates of all modes. There could be variations in modal frequencies between undamaged samples due to non-identical geometry, but the change in decay rate is predominantly a function of the structural integrity. The samples with crack have a larger decay rate, or higher values of λ .

A time-frequency representation (TFR), such as spectrogram, of a response signal as in Equation (1) would reveal the signal components and their time envelopes. For example, Fig. 4 shows the spectrogram of $x(t) = e^{-2t} \sin(2\pi 20t) + e^{-\frac{1}{2}t} \sin(2\pi 40t)$. A spectrogram $X(t, f)$ for a signal $x(t)$ is computed as [10]

$$X(t, f) = \left| \int_{-\infty}^{\infty} x(\tau) w(\tau - t) e^{-j2\pi f \tau} d\tau \right|^2, \quad (2)$$

where $w(\tau)$ is the window function, which in this application was a rectangular window with a much smaller duration than the actual signal. Spectrogram represents the near-instantaneous energy at all frequencies in the signal. The reader must note that any other TFR [10], [11] could be used for this application, but we chose spectrogram for its computational simplicity.

C. Feature Extraction

As indicated earlier, a joint representation of frequencies in the acoustic signature and their decay rates sets apart a healthy sample from a damaged one. Since $X(0, f)$ is the spectrum at the initial time, it was used to determine the K significant frequencies f_1, f_2, \dots, f_K . The time varying energy around each frequency is then computed

$$E_k(t) = \int_{f_k - \Delta f}^{f_k + \Delta f} X(t, \omega) d\omega, \quad \forall k = 1, \dots, K, \quad (3)$$

where Δf the sum of half main lobe width and one side lobe width of the window $w(\tau)$. Subsequently, the decay rate λ_k for all $k = 1, \dots, K$ are estimated using linear least squares



Fig. 5. Experimental setup.

on the envelope of E_k . The features representing a sample is a set of vectors

$$\mathbb{Y} = \left\{ \mathbf{y}_k | \mathbf{y}_k = \begin{bmatrix} f_k \\ \lambda_k \end{bmatrix}; k = 1, \dots, K \right\}. \quad (4)$$

D. Damage Detection

A Gaussian class conditional density function was used to model each of the two classes, healthy and damaged. Unlike a linear discriminant function, a quadratic classifier allows modeling each class with a unique covariance matrix. In [12] it has been shown that the performance of classifiers depend strongly on the inherent pattern in the data. The multinormal nature of our feature-set obtained from acoustic data [13] motivated the use of quadratic discriminant analysis (QDA) [14].

This method adheres to the training-testing paradigm. In the training phase, the mean $\bar{\mathbf{y}}_i$ and covariance matrix \mathbf{S}_i of the i th class ($i = 1, 2$) is computed. In the testing phase, a quadratic score function for each features \mathbf{y}_k from a test sample is calculated using

$$q_i(\mathbf{y}_k) = -\frac{1}{2} \log |\mathbf{S}_i| - \frac{1}{2} (\mathbf{y}_k - \bar{\mathbf{y}}_i)' \mathbf{S}_i^{-1} (\mathbf{y}_k - \bar{\mathbf{y}}_i), \quad (5)$$

$$\forall i = \{1, 2\},$$

assuming that both the classes are equally likely. This test sample is then classified using majority voting of the classification of each of the K features

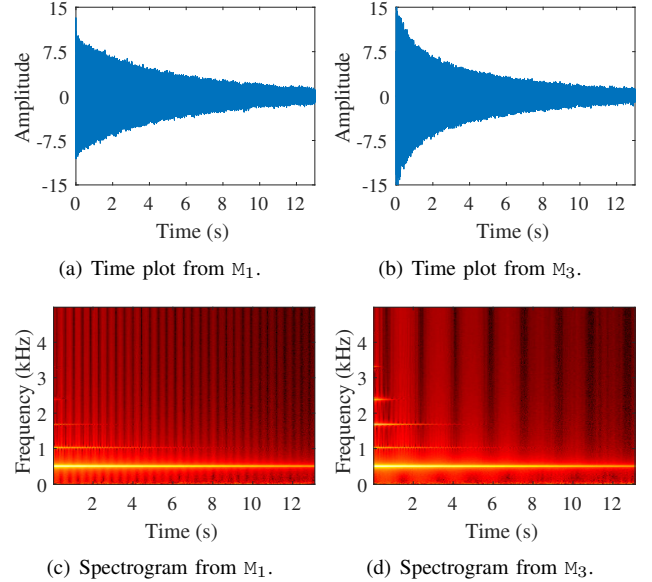
$$\mathcal{C} = \operatorname{argmax}_{c \in \{1, 2\}} \sum_{k=1}^K \delta \left(\left(\operatorname{argmax}_{i \in \{1, 2\}} q_i(\mathbf{y}_k) \right), c \right), \quad (6)$$

where $\delta(\cdot, \cdot)$ is the Kronecker delta function.

III. EXPERIMENTAL SETUP AND DATA COLLECTION

The experimental setup is shown in Fig. 5. A clutch housing sample was secured by the stem in a custom fixture. There were two microphones MIC1 and MIC2, one on each side. The black horizontal bar designates a pivot point till which the hanging weight was pulled before release. Once released, the weight would swing and hit the sample, generating a ping. The weight was arrested after the first ping. Using the pivot point ensured a consistent pinging force. Each ping generated two response signals simultaneously, one from each microphone.

There were ten samples available for experimentation, L_1 , L_2 , L_3 , L_4 , M_1 , M_2 , M_3 , S_1 , S_2 , and S_3 . The labels L, M and

Fig. 6. Acoustic response (normalized to unit energy) from pinging M_1 (healthy) and M_3 (cracked).

S denote groups with large, medium and small amount of material removed, respectively, for load balancing. Damage was induced in one sample from each group, L_4 , M_3 , and S_1 . It must be noted that L_1 had an anomaly and was marked down as one that did not meet the manufacturing quality standards, though it did not have any visible damage. The lack of any apparent damage motivated us to include L_1 in the healthy set.

Experiments were conducted in two folds. The first one used multiple signals from two known samples to test the classifier, and to understand the variability between the microphone signals. The second test was designed to be more representative of a manufacturing end of line inspection. In a manufacturing end of line testing, it would be practical to obtain one response signal from each sample produced, and compare that against a very limited training set from an independent manufacturing batch. Thus, in the second test, one signal from each of the ten samples were used. Two samples were used for training and eight samples for testing.

For the first experiment, we acquired 28 responses from M_1 and 24 responses from M_3 , using each of the two microphones, MIC1 and MIC2, simultaneously sampled at 10 kHz. We investigated frequencies up to 50 kHz, but did not find any compelling features beyond 5 kHz. While there was a subtle difference between a healthy and a cracked sample in the envelopes of the time plots as shown in Fig. 6(a) and (b), the spectrograms in Fig. 6(c) and (d) provided a clearer distinction. Each spectrogram was generated with 512 frequency points using a rectangular window of 512 time-samples, advancing by 1 time-sample. Since the key differences were over 1 kHz, twenty ($K = 20$) most significant frequencies above 1 kHz were used to create the discriminative features \mathbb{Y} . Discarding the frequencies

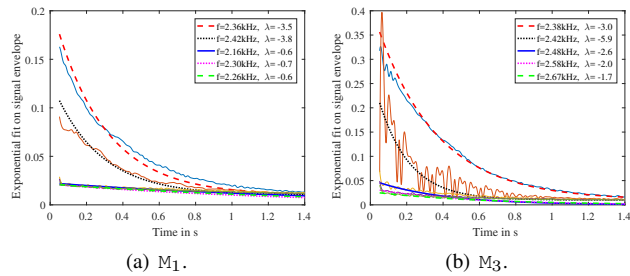
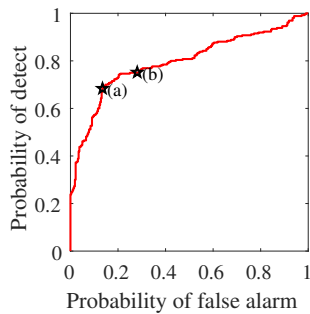
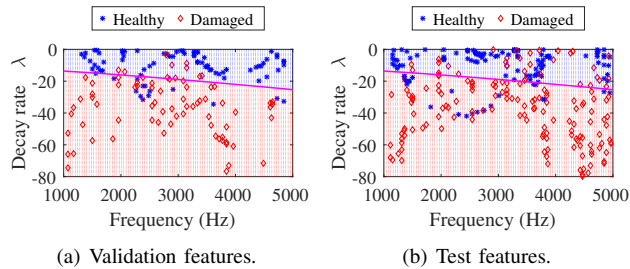
Fig. 7. Exponential fit for estimating λ .

Fig. 8. Quadratic discriminant classifier result.

below 1 kHz also helped in eliminating the effect of the dominant modes, common to the healthy and the damaged signals [15]. Fig. 7 shows exponential fit of the energy envelop corresponding to a few of the frequencies that were used to estimate the corresponding λ s.

The classes were trained using MIC1 data; 12 from M_1 and 11 from M_3 . The corresponding data from MIC2 were used for validation. The remaining signals from MIC1 were used for testing. Fig. 8(a) and (b) shows a scatter of the features y_m from the validation and test set, respectively, of both the classes, along with the decision boundary. Fig. 8(c) shows the receiver operating characteristic (ROC) curve of the final classifier using Equation (6). There are two points on the ROC curve, (a) and (b) marked. The confusion matrices corresponding to these points are presented in Table I. Point (b) would be a preferred classifier since it did not miss any damaged samples, while maintaining a low total error. During this experiment, we established that the features extracted from the two microphones were nearly identical and using any one would yield similar results.

For the second experiment, only one signal per microphone

TABLE I
CONFUSION MATRIX FROM ROC POINTS IN FIG. 8(C)

ROC points		Healthy	Damaged
(a)	Healthy	16	0
	Damaged	4	9
(b)	Healthy	14	2
	Damaged	0	13

TABLE II
PERFORMANCE SUMMARY.

Sample ID	True Class	Estimated Class
L_1	Healthy	Damaged
L_2	Healthy, used for training/validation	
L_3	Healthy	Healthy
L_4	Damaged	Damaged
M_1	Healthy	Healthy
M_2	Healthy	Healthy
M_3	Damaged	Damaged
S_1	Damaged, used for training/validation	
S_2	Healthy	Healthy
S_3	Healthy	Healthy

per sample was recorded for each of the ten samples. Our goal was to train on the minimum number of samples, and in this case we chose 1 from each class. Responses from MIC1 of L_2 and S_1 were used to train. The responses from MIC2 of these samples were used for validation. The responses of the remaining samples were used for testing (there was no discrepancy when using either MIC1 or MIC2). Table II summarizes the outcome of this experiment. While this method did not miss any damaged samples, it mislabeled one healthy sample, out of the six available, as damaged.

IV. CONCLUSION

In this paper, a simple classifier is presented for structural damage detection in a metal-cast automotive component, such as a clutch housing, that has non-identical geometry between samples to satisfy functional requirements. The samples were pinged using a weight and the response was recorded using two microphones. Joint time-frequency representation was an essential tool in identifying the underlying structure in these acoustic response signals obtained from the samples. A two-dimensional feature composed of the significant frequencies (that do not correspond to the dominant vibration modes), and the decay rates of the energy at those frequencies, was a successful discriminating factor. There are other methods that could be used for feature creation, like matching and basis pursuit decomposition but, that might require a higher computation time.

The method of pinging for acoustic response is a global damage detector since the classifying features are not sensitive to the location of the microphones. The distance of the microphone from the samples would impact the amplitude

of recorded acoustic signal but, the selected frequency and decay rate features are immune to such variation.

We could obtain successful classification using a QDA with minimal training. Note that the QDA is a simple classifier with minimum error in a Gauss-Gauss detection scenario, which was a fair assumption in our dataset. QDA is mathematically similar to maximum a posteriori probability detector. When a complete knowledge on the data is not available, one could use hypothesis testing approaches like generalized likelihood ratio test, Wald test or Rao test [16].

The non-destructive damage inspection technique outlined here could be deployed as an end of line inspection in large volume manufacturing of components, like the clutch housing. However, this method requires rigorous training, validation, and sensitivity analysis on the intensity of damage, before it could meet the standards for automotive component manufacturing.

REFERENCES

- [1] J. Kim, G. Yang, L. Udpa, and S. Udpa, "Classification of pulsed eddy current gmr data on aircraft structures," *NDT & E International*, vol. 43, no. 2, pp. 141–144, 2010.
- [2] N. Goldfine, A. Washabaugh, Y. Sheiretov, and M. Windoloski, *Eddy-Current Methods*, John Wiley & Sons, Ltd, 2009.
- [3] M. Şimşira and A. Ankara, "Comparison of two non-destructive inspection techniques on the basis of sensitivity and reliability," *Materials & Design*, vol. 28, no. 5, pp. 1433 – 1439, 2007.
- [4] A. J. McEvily, "Failures in inspection procedures: case studies," *Engineering Failure Analysis*, vol. 11, no. 2, pp. 167 – 176, 2004, Papers presented at the International Conference on Failure Analysis {ICFA}.
- [5] R. Polikar, L. Udpa, S. Udpa, and T. Taylor, "Frequency invariant classification of ultrasonic weld inspection signals," *IEEE transactions on ultrasonics, ferroelectrics, and frequency control*, vol. 45, no. 3, pp. 614–625, 1998.
- [6] G. Park, H. Sohn, C. R. Farrar, and D. J. Inman, "Overview of piezoelectric impedance-based health monitoring and path forward," 2003.
- [7] H. Sohn and C. R. Farrar, "Damage diagnosis using time series analysis of vibration signals," *Smart materials and structures*, vol. 10, no. 3, pp. 446, 2001.
- [8] H. Sohn, C. R. Farrar, N. F. Hunter, and K. Worden, "Structural health monitoring using statistical pattern recognition techniques," *Journal of dynamic systems, measurement, and control*, vol. 123, no. 4, pp. 706–711, 2001.
- [9] S. W. Doebling, C. R. Farrar, and M. B. Prime, "A summary review of vibration-based damage identification methods," *Identification Methods, The Shock and Vibration Digest*, vol. 30, pp. 91–105, 1998.
- [10] L. Cohen, "Time-frequency distributions-a review," *Proceedings of the IEEE*, vol. 77, no. 7, pp. 941–981, Jul 1989.
- [11] A. Papandreou-Suppappola, R. L. Murray, Byeong-Gwan Iem, and G. F. Boudreaux-Bartels, "Group delay shift covariant quadratic time-frequency representations," *IEEE Transactions on Signal Processing*, vol. 49, no. 11, pp. 2549–2564, Nov 2001.
- [12] S. J. Dixon and R. G. Brereton, "Comparison of performance of five common classifiers represented as boundary methods: Euclidean distance to centroids, linear discriminant analysis, quadratic discriminant analysis, learning vector quantization and support vector machines, as dependent on data structure," *Chemometrics and Intelligent Laboratory Systems*, vol. 95, no. 1, pp. 1–17, 2009.
- [13] S. Rippengill, K. Worden, K. M. Holford, and R. Pullin, "Automatic classification of acoustic emission patterns," *Strain*, vol. 39, no. 1, pp. 31–41, 2003.
- [14] M. C. Fulcomer, P. H. Schonemann, and G. Molnar, "Program abstracts / algorithms — classification by linear and quadratic discriminant scores," *Behavior Research Methods & Instrumentation*, vol. 6, no. 4, pp. 443 – 445, 1974.
- [15] D. Chakraborty, N. Kovvali, J. Wei, A. Papandreou-Suppappola, D. Cochran, and A. Chattopadhyay, "Damage Classification Structural Health Monitoring in Bolted Structures Using Time-frequency Techniques," *Journal of Intelligent Material Systems and Structures, special issue on Structural Health Monitoring*, vol. 20, no. 11, pp. 1289–1305, July 2009.
- [16] S. M. Kay, *Fundamentals of statistical signal processing. [Volume II]. , Detection theory*, Prentice Hall signal processing series. Prentice Hall, Upper Saddle River (N.J.), 1998.